

Growth of hydrogenated Si clusters using a quadrupole ion trap

Toshihiko Kanayama^a and Hirohiko Murakami^b

^aJoint Research Center for Atom Technology -National Institute for Advanced Interdisciplinary Research,

^bJoint Research Center for Atom Technology -Angstrom Technology Partnership,
1-1-4 Higashi, Tsukuba-shi, Ibaraki 305, Japan

^aElectrotechnical Laboratory, 1-1-4 Umezono, Tsukuba-shi, Ibaraki 305, Japan

For the purpose of formation of nanoclusters with a definite atomic structure, a new electrical trapping technique of charged particles has been developed, which allows us to confine, grow and mass-selectively extract cluster ions. In the trap, Si_nH_x^+ clusters were grown from dilute silane gas, where trapped SiH_x^+ ions were allowed to react with neutral silane molecules or radicals. The mass spectra were measured for $n=1-10$ and several particularly stable compositions were observed, including the compact structures with less H atoms and the bulk-like tetrahedrally coordinated structures with H-terminated dangling bonds.

1. INTRODUCTION

The electromagnetic trapping technique of charged particles [1-3] may have profound potential for material processing. While it has already been used for observation of reactions of confined ions with neutral molecules [4-10], no particular method has ever been proposed specifically for the purpose of preparation of well defined clusters. To this end, we have developed a new type of ion trap aiming at growth of nanometric composite clusters under controlled conditions [11]. Here we describe the principle of our trap/growth equipment and discuss results of our growth experiments of Si_nH_x^+ clusters starting from SiH_4 [12].

2. ION TRAP

The basic structure of our ion trap [11] is shown in Fig.1. The purpose of this equipment is to confine ions in a definite region and grow them by supplying neutral atoms or molecules until the mass reaches a predetermined value. The main part is a set of linear quadrupole, whose role is to hold ions with a wide range of mass values in the outside region surrounding it. The ion is trapped by the electrostatic force from the dc voltage V_{dc} applied commonly to

the electrodes. The quadrupole field generated from the ac voltage V_{ac} acts as a repulsive force to the ion, when time averaged [13]. The balanced position of the repulsive force and the dc attractive force r_0

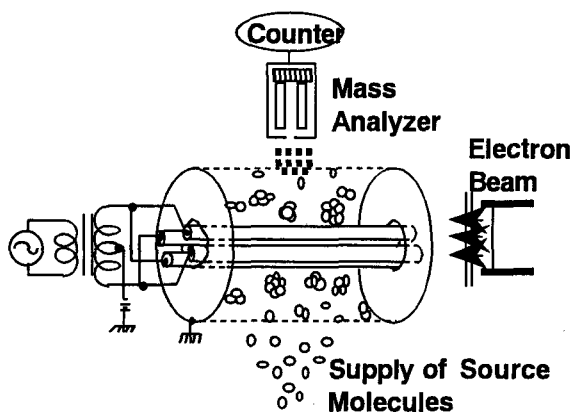


Figure 1. Schematic structure of the present ion trap. Ions are trapped around a set of quadrupole electrodes, to which ac voltages of opposite phases with a common dc bias are connected. The trapping region is defined by wrapping the quadrupole by the cage at the ground potential.

depends on the ion mass m , as

$$r_0 \sim (qV_{ac}^2/m\omega^2V_{dc})^{1/6}, \quad (1)$$

where q is the ion charge and ω is the angular frequency of the ac. The equation of motion in the above field is characterized by the dimensionless parameter k

$$k \sim (V_{ac}m\omega^2/qV_{dc}^2)^{1/3}, \quad (2)$$

and our numerical simulation [11] indicated that the trapping motion is stable if $k > 10$. These relations ensure that the trap can confine particles with a wide range of mass values. Furthermore, as the particle gets heavier, its position comes near to the electrodes. Thus it is possible to pull out the particle mass-selectively into the internal region and finish the growth.

The above features were verified by trapping experiments of inert gas ions. The quadrupole used consisted of four cylinders with 1 cm diameter, to which ac voltages of ~ 100 kHz were connected with a common dc bias of -1.5 V. Figure 2 shows that the trap can confine ions with largely different masses such as Xe^+ and He^+ for several seconds without the need for adjusting the parameters. It has also been experimentally verified that the present trap has the ability to extract the ions mass-selectively through the internal region of the quadrupole. For this purpose, the ion channel was made between the external and the internal regions by cutting the quadrupole at the three quarter length, while in Fig.1 the quadrupole penetrates through the ground cage. The ion can enter into the internal region through the cut end only when it has a mass larger than a specific value determined by the ac voltage and frequency. Thus, this feature allows us to selectively pick up clusters grown to a predetermined mass by tuning ω with keeping other ions confined in the external region.

3. GROWTH OF $Si_nH_x^+$ CLUSTERS

We have applied the above trapping technique to formation of hydrogenated Si clusters. As a source material, SiH_4 gas of $\sim 10^{-4}$ Pa and He buffer of $\sim 10^{-3}$ Pa were introduced into the trapping region and irradiated with electrons of 100 eV for ~ 1 s. The

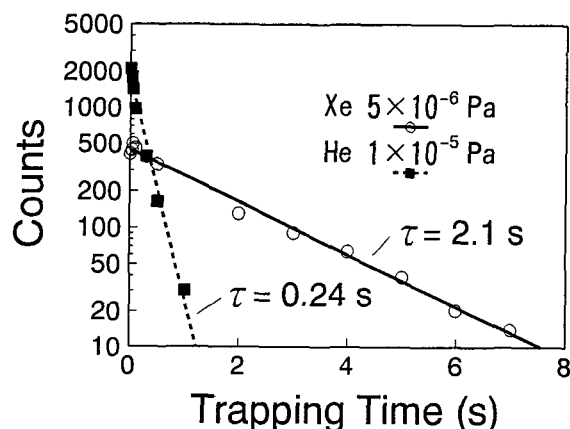


Figure 2. Results of trapping experiments of Xe and He ions. Ions are produced in the trapping region by the pulsed electron beam and counted through the extraction electrode after a predetermined trapping time. The number of ions extracted from the trap is plotted against the time interval between the ionization and the extraction. Values of $1/e$ lifetime τ are also shown.

SiH_x^+ ions generated were confined in the trap and allowed to grow to $Si_nH_x^+$ through reaction with neutral SiH_x radicals which were also formed by the electron irradiation. After being confined for additional interval of ~ 0.1 s from the electron irradiation, produced clusters were extracted from the trap and were analyzed by a quadrupole mass spectrometer. In the trap, confined ions are vibrated by the ac trapping field and the resultant vibration energy of ~ 1 eV partly turns into the internal energy of the ions through collisions with ambient He atoms. Consequently, trapped ions always receive some annealing effect.

Mass spectra of formed $Si_nH_x^+$ ($n=1-7$) clusters are shown in Fig.3. It is seen that when the trapping time is increased from 10 to 100 ms, the population of the hexamer ions grows up while that of the monomer almost disappears. This shows that the growth reaction proceeds in this time range. In contrast, no cluster formation was observed unless the trap was operated. This is because the reactant density is very low in the present experiment and the ions are lost before the growth reactions occur.

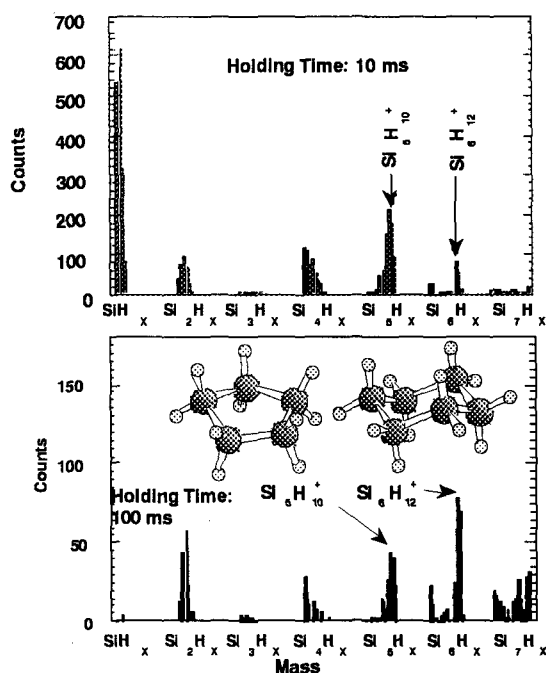


Figure 3. Histogram showing the product distributions for Si_nH_x^+ ($n=1-7$) clusters for holding time of 10 ms (upper) and 100 ms (lower). Two peaks are seen at $\text{Si}_5\text{H}_{10}^+$ and $\text{Si}_6\text{H}_{12}^+$, indicating that these clusters are particularly stable. Their structures are inferred from the compositions to be the five-membered and the six-membered rings consisting of SiH_2 , as shown in the inset.

The observed mass distribution is not uniform but characterized by peaks at the several mass values. The most prominent one is at Si_6H_{12} or $\text{Si}_6\text{H}_{13}^+$ in the figure, indicating that this cluster ion is particularly stable. The observed composition suggests that the $\text{Si}_6\text{H}_{12}^+$ cluster has the form of a six-membered ring consisting of SiH_2 , as shown in the inset. In addition to the hexamer, the second largest is $\text{Si}_5\text{H}_{10}^+$, the structure of which is also inferred to be a SiH_2 ring. Although formation of Si_nH_x clusters are frequently observed in silane plasmas and their mass spectra were discussed by several authors [14-20], no particular preference has been observed in the hydrogen content x . We believe that the reason why only the stable structures survive in the present experiment is due to the annealing effect mentioned above [12].

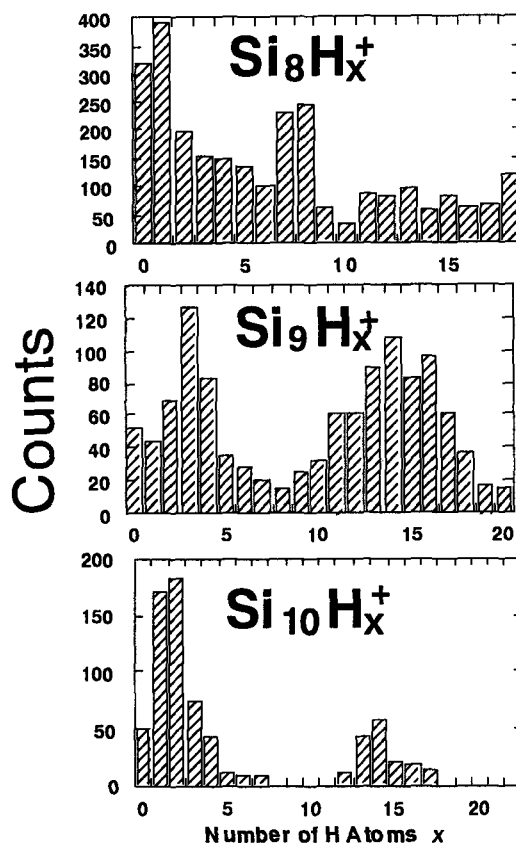


Figure 4. Mass spectra for Si_nH_x^+ ($n=8-10$) clusters. While the spectrum is widely spread for $n=8$, it shrinks to two peaks when n goes up through 9 to 10. This indicates that there are two stable structures for $n=10$: one containing 12-17 H atoms and the other with 0-4.

We observed intriguing features in mass spectra for Si_nH_x^+ ($n=8-10$) clusters shown in Fig.4. While the spectrum is widely spread for $n=8$, it shrinks to two peaks when n goes up through 9 to 10. This indicates that there are two different kinds of stable structures for $n=10$: one with $x=0-4$ and the other with $x=12-17$. The one with a smaller number of H atoms probably has the compact structure theoretically predicted [21-23] for Si_{10} clusters, shown in Fig.5 (a). This structure maximizes the coordination number of Si atoms to reduce the dangling bonds within an energetic allowance. Interestingly, the second composition of $x=12-17$ coincides with the bulk fragment structure shown in

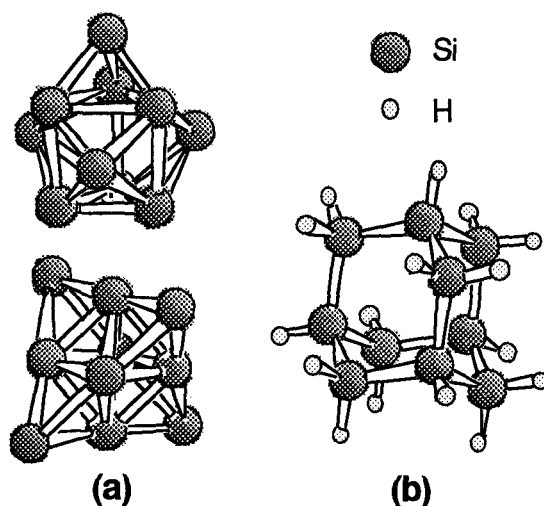


Figure 5. Possible structures for Si_{10}H_x . The compact structures on the left-hand side (a) are predicted for Si_{10} without H atoms by theoretical studies [21,22]. The one on the right-hand side (b) is a bulk fragment of the diamond structure with 16 H atoms on the periphery.

Fig.5 (b). In the bulk-like diamond structure, ten atoms form three intersecting six-membered rings. When this structure is cut out from the bulk, there remain 16 dangling bonds and this number of H atoms are required to terminate them. We attribute the peak at $x = 12-17$ to this hydrogen terminated bulk-fragment structure.

4. CONCLUSION

Hydrogenated Si clusters were grown in a quadrupole ion trap recently developed for this purpose, resulting in several characteristic stable compositions. Their structures are inferred to be the compact structures with less H atoms and the bulk-like tetrahedrally coordinated structures with H-terminated dangling bonds. We believe that these results confirm the validity of the present trap as a cradle for nanostructure formation.

ACKNOWLEDGMENT

This work, partly supported by NEDO, was performed in JRCAT under the joint research

agreement between the National Institute for Advanced Interdisciplinary Research (NAIR) and the Angstrom Technology Partnership (ATP).

REFERENCES

1. H.G. Dehmelt, in *Advances in Atomic and Molecular Physics* (Academic Press, New York and London, 1967) vol.3, p.53.
2. R.F. Wuerker, H. Shelton and R.L. Langmuir, *J. Appl. Phys.* **30** (1959) 342.
3. P.H. Dawson and N.R. Whetten, *J. Vac. Sci. Technol.* **5** (1968) 1.
4. M.L. Mandich, W.D. Reents, Jr. and V.E. Bondybey, *J. Phys. Chem.* **90** (1986) 2315.
5. W.R. Creasy, A. O'Keefe and J.R. McDonald, *J. Phys. Chem.* **91** (1987) 2848.
6. J.M. Alford, P.E. Williams, D.J. Trevor and R.E. Smalley, *Int. J. Mass Spectrom. Ion Process.* **72** (1986) 33.
7. J.L. Elkind, J.M. Alford, F.D. Weiss, R.T. Laaksonen and R.E. Smalley, *J. Chem. Phys.* **87** (1987) 2397.
8. J.M. Alford, R.T. Laaksonen and R.E. Smalley, *J. Chem. Phys.* **94** (1991) 2618.
9. M.L. Mandich and W.D. Reents, Jr., *J. Chem. Phys.* **96** (1992) 4233.
10. N. Watanabe, H. Shiromaru, Y. Negishi, Y. Achiba, N. Kobayashi and Y. Kaneko, *Z. Phys.* **D26** (1993) S252.
11. T. Kanayama, *Jpn. J. Appl. Phys.* **33** (1994) L1792.
12. H. Murakami and T. Kanayama, *Appl. Phys. Lett.* **67** (1995) 2341.
13. L.D. Landau and E.M. Lifshitz, *Mechanics* (Pergamon, Oxford, 1960) Chap.5.
14. I. Haller, *Appl. Phys. Lett.* **37** (1980) 282.
15. T. P. Martin and H. Schaber, *J. Chem. Phys.* **83** (1985) 855.
16. H. A. Weakliem, R. D. Estes and P. A. Longeway, *J. Vac. Sci. Technol.* **A5** (1987) 29.
17. M.L. Mandich, W.D. Reents, Jr., and M.F. Jarrold, *J. Chem. Phys.* **88** (1988) 1703.
18. M.L. Mandich, W.D. Reents, Jr., and K.D. Kolenbrander, *J. Vac. Sci. Technol.* **B7** (1989) 1295.
19. M.L. Mandich, W.D. Reents, Jr., and K.D. Kolenbrander, *J. Chem. Phys.* **92** (1990) 437.
20. M.L. Mandich and W.D. Reents, Jr., *J. Chem. Phys.* **95** (1991) 7360.
21. K. Raghavachari and C. M. Rohlfing, *J. Chem. Phys.* **89** (1988) 2219.
22. K. Raghavachari, *Phase Trans.* **24-26** (1990) 61, and references therein.
23. M. F. Jarrold, *Science* **252** (1991) 1085.